Transient growth, edge states, and repeller in rotating solid and fluid

Kevin Ha, Jean-Marc Chomaz, Sabine Ortiz

Transient growth, edge states and repeller in rotating solid and fluid

Kevin Ha, Jean-Marc Chomaz, and Sabine Ortiz
LadHyX, Ecole Polytechnique, CNRS UMR 7646, 91128 Palaiseau Cedex, France and
IMSIA, ENSTA Paristech, EDF/CNRS/CEA/ENSTA UMR 9219, F-91762 Palaiseau Cedex, France

For the classical problem of the rotation of a solid, we show a somehow surprising behavior involving large transient growth of perturbation energy that occurs when the moment of inertia associated to the unstable axis approaches the moment of inertia of one of the two stable axes. In that case, small but finite perturbations around this stable axis may induce a total transfer of energy to the unstable axis leading to relaxation oscillations where the stable and unstable manifolds of the unstable axis play the role of a separatrix, an edge state. For a fluid in solid body rotation, a similar linear and nonlinear dynamics apply to the transfer of energy between three inertial waves respecting the triadic resonance condition. We show that the existence of large transient energy growth and of relaxation oscillations may be physically interpreted as in the case of a solid by the existence of two quadratic invariants, the energy and the helicity in the case of a rotating fluid. They occur when two waves of the triad have helicities that tend towards each other, when their amplitudes are set such that they have the same energy. We show that this happens when the third wave has a vanishing frequency which corresponds to a nearly horizontal wavevector. An inertial wave, perturbed by a small amplitude wave with a nearly horizontal wavevector, will then be periodically destroyed, its energy being transferred entirely to the unstable wave, although this perturbation is linearly stable, resulting in relaxation oscillations of wave amplitudes. In the general case, we show that the dynamics described for particular triads of inertial waves is valid for a class of triadic interactions of waves in other physical problems, where the physical energy is conserved and is linked to the classical conservation of the so-called pseudomomentum, which singles out the role of waves with vanishing frequency.

ROTATING RIGID BODY

The motion of a solid is a well-studied problem. For a non-symmetric rigid body, the rotation around the two axes with the highest and the smallest moments of inertia are stable whereas the intermediate axis is unstable resulting in the so-called tennis racket effect [1] (see video at `https://www.youtube.com/watch?v=1VPfZ_XzisU`). We reconsider this classic example and show that surprising phenomena occur also for a rotation around a stable axis when the smallest or the highest moment of inertia of the solid J_1 or J_0 gets close to the intermediate one J_2 and discuss the extension to conservative waves systems.

The rotation of a rigid body in the reference frame with its axes fixed to the body obey to [2] :

$$\frac{dM_0}{dt} = \left(\frac{1}{J_2} - \frac{1}{J_1}\right) M_2 M_1$$
$$\frac{dM_1}{dt} = \left(\frac{1}{J_0} - \frac{1}{J_2}\right) M_0 M_2 \qquad (1)$$
$$\frac{dM_2}{dt} = \left(\frac{1}{J_1} - \frac{1}{J_0}\right) M_1 M_0$$

where $\mathbf{M} = (M_0, M_1, M_2)^{\mathrm{T}}$ is the angular momentum vector and $0 < J_1 < J_2 < J_0$ are the moments of inertia. Equations (1) conserve the total energy $\mathcal{E}$ and the total momentum $\mathcal{M}$ (with the change of variables $M'_n = M_n/\sqrt{2J_n}$) :

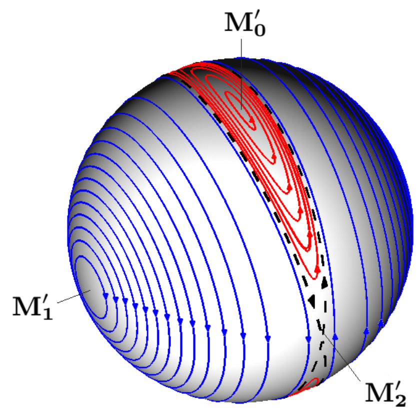

FIG. 1. Trajectories on the sphere unity $\mathcal{E} = 1$ in the (M'_0, M'_1, M'_2) space with $J_2 = (1-\varepsilon)J_0$, $\varepsilon = 2.10^{-2}$, $J_1 = (1-\Sigma)J_0$ and $\Sigma = 0.9$. The point $\mathbf{M'_1} = (0,1,0)^{\mathrm{T}}$ is stable and close trajectories around $\mathbf{M'_1}$ are plotted in blue, $\mathbf{M'_0} = (0,0,1)^{\mathrm{T}}$ is stable too and close trajectories around $\mathbf{M'_0}$ are in red.

$$\mathcal{E} = \sum_n M'^2_n, \quad \mathcal{M}^2 = \sum_n 2J_n M'^2_n \qquad (2)$$

In a (M'_0, M'_1, M'_2) space, the energy is the Euclidean norm and trajectories are given by the intersection of the sphere of energy $\mathcal{E}$ and constant momentum ellipsoids with $\mathcal{M}^2$ between $2J_1\mathcal{E}$ and $2J_0\mathcal{E}$. By rescaling the angular momentum, we may set $\mathcal{E} = 1$. Figure 1 represents those intersections for different values of $\mathcal{M}^2$ when $J_2 = (1-\varepsilon)J_0$ with $\varepsilon = 2.10^{-2}$ and $J_1 = (1-\Sigma)J_0$ with

$\Sigma = 0.9$. On the sphere, the point $\mathbf{M_2'} = (0,0,1)^{\mathrm{T}}$ is unstable and surrounded locally by hyperbolic trajectories, the points $\mathbf{M_1'} = (0,1,0)^{\mathrm{T}}$ and $\mathbf{M_0'} = (1,0,0)^{\mathrm{T}}$ are stable and surrounded by ellipses (in blue and red). The two basins of solutions nutating around $\mathbf{M_1'}$ in blue or $\mathbf{M_0'}$ in red are separated by the separatrix given by $\mathcal{M}^2 = 2J_2$

Linear perturbations $(m_0', m_1', m_2')^{\mathrm{T}}$ around the stable point $\mathbf{M_0'}$ belong to the tangent plane $\mathbf{m}' = (m_1', m_2')^{\mathrm{T}}$ since $dm_0'/dt = 0$ at leading order :

$$\frac{d\mathbf{m}'}{d\tau} = \mathcal{L}\mathbf{m}' \quad \text{with} \quad \mathcal{L} = \begin{pmatrix} 0 & -\varepsilon \\ \Sigma & 0 \end{pmatrix} \tag{3}$$

with $\tau = t\sqrt{2/(1-\varepsilon)(1-\Sigma)J_0}$. We define the optimal perturbation energy gain G as :

$$G(\tau) = \max_{e(0)=1} e(\tau) \tag{4}$$

where $e = m_1'^2 + m_2'^2$ is the energy of the perturbation. When $\varepsilon \neq \Sigma$, the evolution operator $\mathcal{L}$ is nonnormal with respect to the classical Euclidean inner product, its associated norm being the energy e, and $\mathcal{L}\mathcal{L}^{\mathrm{T}} \neq \mathcal{L}^{\mathrm{T}}\mathcal{L}$. The energy gain G is plotted as a function of time on figure 2. The gain is periodic and when ε decreases, the maximum value of G, $G_{\max} = \Sigma/\varepsilon$, and the period of oscillations $T = 2\pi/\sqrt{\varepsilon\Sigma}$ increase. This transient growth corresponds to the elongated elliptic trajectories around the stable point $\mathbf{M_0'}$ on figure 2.

For finite initial amplitude, the trajectories are no more on the tangent plane but on the sphere meaning that to conserve energy, $\mathbf{M_0'}$ has to depart from unity. They keep being closed around the point $\mathbf{M_0'}$ until they pass the separatrix that links the saddle $\mathbf{M_2'}$ and $-\mathbf{M_2'}$ and crosses the $M_2' = 0$ plane on the point $\mathbf{M}_\varepsilon' = (\sqrt{1-\varepsilon/\Sigma}, \sqrt{\varepsilon/\Sigma}, 0)^{\mathrm{T}}$. Therefore, a perturbation of the point $\mathbf{M_0'}$ along the $\mathbf{M_1'}$ axis of perturbation energy ε/Σ will trigger a motion no more nutating around $\mathbf{M_0'}$ but around $\mathbf{M_1'}$ with periodic extinction of the rotation around the point $\mathbf{M_0'}$. The trajectories show relaxation with extremely large time spent around the unstable point $\mathbf{M_2'}$ that acts as a repeller and transient short passage close to the stable point $\mathbf{M_0'}$.

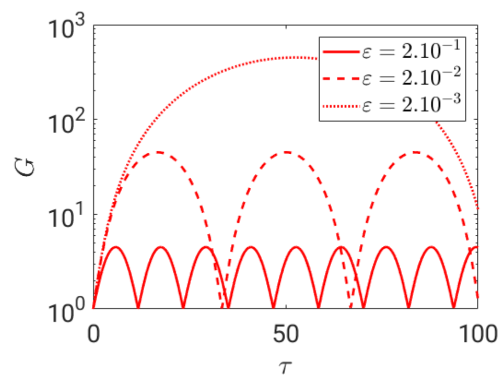

FIG. 2. Energy gain G defined in (4) as a function of time τ for the linearized problem around the stable point $\mathbf{M_0'} = (0,0,1)^{\mathrm{T}}$ for $\Sigma = 0.9$ and $\varepsilon = 2.10^{-1}$ (continuous line), $\varepsilon = 2.10^{-2}$ (dashed line) and $\varepsilon = 2.10^{-3}$ (dotted line).

ROTATING FLUID

Similar transient growth mechanism and nonlinear separatrix concern other conservative systems and we consider here the case of resonant triad of inertial waves in rotating fluids [3]. When an incompressible, inviscid fluid is in solid body rotation at angular velocity Ω along the z axis, the Coriolis force acts as a conservative restoring force and is associated with the propagation of waves given by the dispersion relation :

$$\left(\frac{\omega}{f}\right)^2 = \left(\frac{k_z}{k}\right)^2 \tag{5}$$

where $f = 2\Omega$ is the Coriolis parameter, $\mathbf{k}$ the wavevector, k its modulus and k_z its vertical component. This dispersion relation is derived linearizing the incompressible rotating Euler equation. When the wave amplitude is not infinitesimal, the Rossby number $Ro = U/(Lf)$, where U and L are the typical velocity and length scale in the wave field, becomes finite. The nonlinearity in the rotating Euler equation being quadratic, three waves $(\omega_0, \mathbf{k}_0)$, $(\omega_1, \mathbf{k}_1)$, $(\omega_2, \mathbf{k}_2)$ independent at leading order in Rossby number will be coupled at the second order if they form a triad :

$$\begin{aligned} \omega_0 + \omega_1 + \omega_2 &= 0 \\ \mathbf{k}_0 + \mathbf{k}_1 + \mathbf{k}_2 &= \mathbf{0} \end{aligned} \tag{6}$$

If we note s_n the sign of the frequency ω_n of the n-th wave, the triadic resonance conditions (6) give by eliminating $\mathbf{k}_2$:

$$s_0\frac{|k_{z0}|}{k_0} + s_1\frac{|k_{z1}|}{k_1} + s_2\frac{|k_{z0}+k_{z1}|}{k_{01}} = 0 \tag{7}$$

where k_0, k_1 and k_{01} are respectively the modulus of $\mathbf{k}_0$, $\mathbf{k}_1$ and $\mathbf{k}_0 + \mathbf{k}_1$. For simplicity, we will assume the plane formed by the three resonant wavevectors to be vertical ($k_{yn} = 0$). In this so-called 2D-3C (two-dimensional, three components) model [4], waves may be defined by their streamfunction with a complex amplitude Ψ_n, the associated velocity along x, y and z being $u_n = -ik_{zn}\Psi_n \exp i(k_{xn}x + k_{zn}z - \omega_n t) + c.c.$, $v_n = -fk_{zn}/\omega_n \Psi_n \exp i(k_{xn}x + k_{zn}z - \omega_n t) + c.c.$ and $w_n = -k_{xn}/k_{zn}u_n$ where *c.c.* indicates the complex conjugate. Formally, the derivation involves a multiscale expansion with the introduction of a slow time scale $T = Rot$, the wave amplitude $\Psi_n(T)$ then being a function of T as in the derivation of the WKB approximation [5]. A second order expansion in Rossby number leads to the amplitude equations for the resonant waves (see [6] for more details). When transforming back the slow time scale T in the primitive time t, those equations read :

$$
\begin{aligned}
\frac{d\Phi_0}{dt} &= \Delta\Gamma(\sigma_2 k_2 - \sigma_1 k_1)\Phi_2^*\Phi_1^* \\
\frac{d\Phi_1}{dt} &= \Delta\Gamma(\sigma_0 k_0 - \sigma_2 k_2)\Phi_0^*\Phi_2^* \\
\frac{d\Phi_2}{dt} &= \Delta\Gamma(\sigma_1 k_1 - \sigma_0 k_0)\Phi_1^*\Phi_0^*
\end{aligned}
\tag{8}
$$

with the change of variable $\Phi_n = k_n \Psi_n/2$, Δ being twice the oriented area of the triangle ($\mathbf{k}_0$, $\mathbf{k}_1$, $\mathbf{k}_2$), $\Delta = k_{x1}k_{z2} - k_{x2}k_{z1}$, $\sigma_n = s_n \mathrm{sign}(k_{zn})$ the vertical orientation of the phase velocity and $\Gamma = (\sigma_0 k_0 + \sigma_1 k_1 + \sigma_2 k_2)/(k_0 k_1 k_2)$. Equations (8) admit three invariants :

$$
\begin{aligned}
\mathcal{E} = \sum_n |\Phi_n|^2, \quad \mathcal{H} = \sum_n 2\sigma_n k_n |\Phi_n|^2, \\
\mathcal{K} = |\Phi_0|\,|\Phi_1|\,|\Phi_2| \sin\varphi
\end{aligned}
\tag{9}
$$

where φ is the phase of $\Phi_0\Phi_1\Phi_2$. $\mathcal{E}$ is the energy, the sum of each wave total energy $|\Phi_n|^2$, and $\mathcal{H}$ the helicity conserved within the triad as discussed in [3]. Only the invariant $\mathcal{K}$, also called Hamiltonian by [7], involves the phases of Φ_n, as discussed in [8]. The analogy with the solid body rotation is direct comparing the quadratic invariants of the two systems with $|\Phi_n|$ playing the role of $|M'_n|$ and k_n the role of the moments of inertia J_n, the differences being that the wave amplitudes Φ_n are complex and that when one σ_n is negative, the helicity $\mathcal{H}$ is not a definite positive form. For simplicity, we study the triad T plotted in black on figure 3 whose helicity signs are all positive i.e. $(\sigma_0, \sigma_1, \sigma_2) = (+,+,+)$ with $k_0 = 1$ by rescaling the space. By rescaling the time, the energy $\mathcal{E}$ is set to unity. Figure 4a) plots in the amplitude space $|\Phi_n|$ the lines where both $\mathcal{E}$ and $\mathcal{H}$ are constant for the triad T. The trajectories lie on the lines of intersection between the unit energy sphere and constant helicity ellipsoid following the same reasoning as for the solid with a separatrix issuing from the unstable wave $(\omega_2, \mathbf{k}_2)$ splitting the modulus space between trajectories oscillating around $(\omega_0, \mathbf{k}_0)$ and around $(\omega_1, \mathbf{k}_1)$. The separatrix is then given by the helicity of wave $(\omega_2, \mathbf{k}_2)$, $\mathcal{H} = 2k_2$ and starts from the point $\mathbf{M'_2} = (0,0,1)^{\mathrm{T}}$ with $\mathbf{M'} = (|\Phi_0|, |\Phi_1|, |\Phi_2|)^{\mathrm{T}}$ and crosses the plane $|\Phi_2| = 0$ at $\mathbf{M}'_\varepsilon = (\sqrt{1-\varepsilon/\Sigma}, \sqrt{\varepsilon/\Sigma}, 0)^{\mathrm{T}}$ with $\varepsilon = 1 - \sigma_2 k_2/(\sigma_0 k_0)$ and $\Sigma = 1 - \sigma_1 k_1/(\sigma_0 k_0)$. The separatrix passes at a distance in perturbation energy of ε/Σ from the point $\mathbf{M'_0} = (1,0,0)^{\mathrm{T}}$ corresponding to the stable wave $(\omega_0, \mathbf{k}_0)$. If for the solid, the lines on the sphere

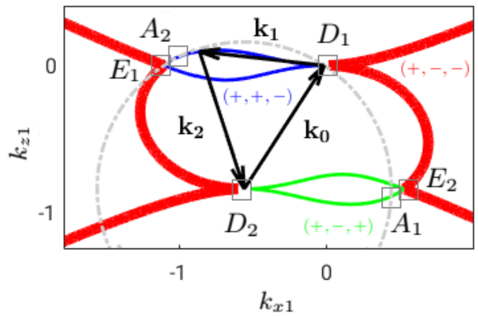

FIG. 3. Resonant triads in the wavevector space $\mathbf{k}_1 = (k_{x1}, k_{z1})$ when the wave $(\omega_0, \mathbf{k}_0)$ is fixed with $s_0 = +1$, $k_0 = 1$ and $\omega_0/f = 0.84$ (value taken from [4]), $\mathbf{k}_0$ being plotted on the figure in black arrow. The unstable branches $(+,-,-)$ are represented in red whereas the stable branches to $(+,-,+)$ and $(+,+,-)$ are represented in blue and green. The unit circle centered on $-\mathbf{k}_0$ is plotted in dashed grey lines. The points (E_1, D_1, A_1) marked with squares indicate triads where $\sigma_2 k_2 \to \sigma_0 k_0 = 1$. (E_2, D_2, A_2) are the symmetric of (E_1, D_1, A_1) by exchanging $\mathbf{k}_1$ and $\mathbf{k}_2$ such that $\sigma_1 k_1 \to \sigma_0 k_0 = 1$. The exemplified triad T ($\mathbf{k}_0 \sim (0.54, 0.84)^{\mathrm{T}}$, $\mathbf{k}_1 \sim (-0.83, 0.1)^{\mathrm{T}}$ and $\mathbf{k}_2 \sim (0.29, -0.94)^{\mathrm{T}}$) is plotted in black.

unity are trajectories traveled in a unique direction, the lines on figure 4a) are only projections of the trajectories in the modulus space. A point on a particular trajectory on figure 4a) is defined by a unique value of the modulus $|\Phi_2|$ ($|\Phi_0|$ and $|\Phi_1|$ being given by the invariants $\mathcal{E}$ and $\mathcal{H}$) but may be realized by different initial values of φ (the phase of the three waves) giving different initial values of the invariant $\mathcal{K}$ between 0 and the initial value of $|\Phi_0||\Phi_1||\Phi_2|$. The conservation of $\mathcal{K}$ imposes that the time evolutions of $|\Phi_2|$ and φ are linked, the vector $(|\Phi_0|, |\Phi_1|, |\Phi_2|)$ being on a particular line on the energy sphere 4a) and the phase φ and the modulus $|\Phi_2|$ being on the trajectory corresponding to different values of $\mathcal{K}$. Figure 4b) shows such a set of trajectories for modulus on the separatrix i.e. for the helicity $\mathcal{H} = 2k_2$, this phase portrait is symmetric with respect to $\varphi = 0$ and only $\varphi \geq 0$ has been plotted. Trajectories where $\mathcal{K} \neq 0$ are closed and never reaches the axis $|\Phi_2| = 0$ or $|\Phi_2| = 1$, nor the axis $\varphi = 0$ or $\varphi = \pi$. The axis $\varphi = 0$ or $\varphi = \pi$ corresponds to the cases where $\mathcal{K} = 0$ with trajectories going from $|\Phi_2| = 1$ to $|\Phi_2| = 0$ and inversely. These cases where $\mathcal{K} = 0$ correspond to the real solutions of the system (8) since it is straightforward to prove that, when the initial conditions Φ_n are real, they stay real at all times and that any initial conditions with $\mathcal{K} = 0$ and non of the modulus $|\Phi_n|$ zero initially is equivalent to a real initial condition. Using the two phases invariances associated to the time and space translation, two of the Φ_n may be initially taken as real, the initial phase of the third Φ_n being then 0 modulo π to respect $\mathcal{K} = 0$. The cases where $\mathcal{K} = 0$ are then strictly equivalent to the solid case and the discussion on the nonlinear effects holds.

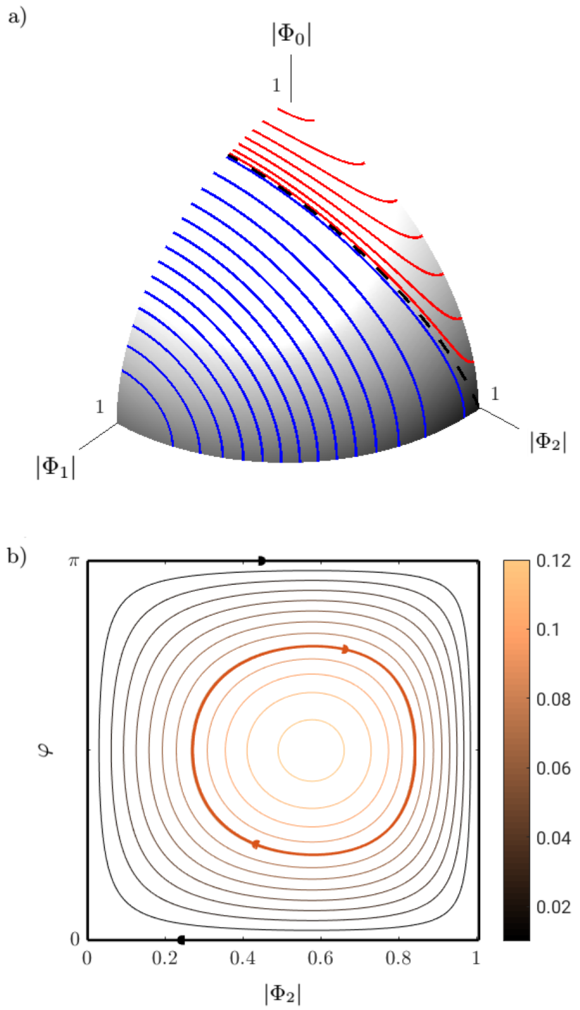

FIG. 4. Trajectories corresponding to the dynamics given by equation (8) for the triad T plotted on figure 3, with $\varepsilon = 1 - \sigma_2 k_2/(\sigma_0 k_0) = 0.02$ and $\Sigma = 1 - \sigma_1 k_1/(\sigma_0 k_0) = 0.16$. a) Projection in the modulus space $(|\Phi_0|, |\Phi_1|, |\Phi_2|)$, trajectories are on the sphere of constant energy $\mathcal{E} = 1$ and corresponds to lines of constant helicity $\mathcal{H}$. b) Trajectories along the separatrix in black dashed lines on a) in the plane $(\varphi, |\Phi_2|)$. Since $\mathcal{K}$ is an invariant, contour plots of $\mathcal{K}$ for values given by the colorbar defines the trajectories. Two trajectories obtained by numerical integration of (8) for different initial conditions are also reported in heavy lines : $(\varphi, |\Phi_2|) = (\pi/4, 0.44)$ in copper, $(0, 0.99)$ in black, and $(\pi, 0.01)$ also in black.

To capture the linear and nonlinear dynamics close to the wave $(\omega_0, \mathbf{k}_0)$ in the triad T, we consider an initial condition such that $|\Phi_0|$ is close to unity and $|\Phi_1|$ and $|\Phi_2|$ small meaning that the invariant $\mathcal{K}$ is small and will be assumed zero to simplify the discussion. For the triad T, the waves $(\omega_0, \mathbf{k}_0)$ and $(\omega_1, \mathbf{k}_1)$ are stable, the wave $(\omega_2, \mathbf{k}_2)$ unstable and $\varepsilon = 1 - \sigma_2 k_2/(\sigma_0 k_0) = 0.02$ and $\Sigma = 1 - \sigma_1 k_1/(\sigma_0 k_0) = 0.17$. Since ε is small compared to Σ, k_2 being close to k_0, large transient growth of the perturbation is possible around the wave $(\omega_0, \mathbf{k}_0)$ corresponding to the elliptic trajectory in red on figure 4a) for which the aspect ratio is scaling like $\sqrt{\varepsilon/\Sigma}$ for a small perturbation amplitude. For larger amplitudes, the ellipses deform when approaching the point $\mathbf{M_2'} = (0, 0, 1)^{\mathrm{T}}$ where $|\Phi_2| = 1$. The separatrix is reached when the helicity approaches the one of the point $\mathbf{M_2'}$, $\mathcal{H} = 2k_2$. As for the solid, trajectories close to the separatrix correspond to relaxation oscillations with a frequency that vanishes on the separatrix. On these relaxation trajectories, the energy in the triad is transferred fast on a time duration proportional to $1/\Sigma$ from the stable wave $(\omega_0, \mathbf{k}_0)$ to the unstable wave $(\omega_2, \mathbf{k}_2)$ and stays close to this unstable wave for a long time. Such a behavior is close to the concept of edge states [9] corresponding to an unstable point, a repeller which still dominates the dynamics, the trajectories being attracted close to that point and leaving it slowly leading to intermittency. For extended flow like boundary layer, the intermittency is in time space and the edge state defines the coherent structuration of the turbulent flow [9]. Here, the edge state is the unstable wave $(\omega_2, \mathbf{k}_2)$ with many initial conditions leading to trajectories that will spend long time close to $(\omega_2, \mathbf{k}_2)$.

Since waves are continuous, it is standard not to study a single triad but families of triads as in [10], [11]. The resonant curves for the vector $\mathbf{k}_0$ fixed and the vector $\mathbf{k}_1$ varying ($\mathbf{k}_2$ being $-\mathbf{k}_0 - \mathbf{k}_1$) solutions of (7) are plotted on figure 3 for $\omega_0/f = 0.84$. The wave $(\omega_0, \mathbf{k}_0)$ is such that $k_0 = 1$ and $s_0 = +1$ (i.e. upward and rightward propagating wave), the other cases being easily deduced by symmetry. The signs (s_0, s_1, s_2) are reported on figure 3 and Hasselmann's criterion [10] states that the wave $(\omega_0, \mathbf{k}_0)$ is unstable on the $(+, -, -)$ branch (in red lines), and stable on the $(+, -, +)$ and $(+, +, -)$ branches (in blue and green lines respectively). On figure 3, the points (E_1, D_1, A_1) are such that $\sigma_2 k_2 = \sigma_0 k_0 = 1$, and their symmetric points when changing $k_2 \leftrightarrow k_1$, (E_2, D_2, A_2), are such that $\sigma_1 k_1 = \sigma_0 k_0 = 1$. Close to (E_1, D_1), $\mathbf{k}_1$ tends to be horizontal and k_1 approaches $2k_{x0}$ and 0 respectively with ω_1 vanishing in the two cases.

The study made for a single triad T extends directly for all the triads on the resonant branches for the wave $(\omega_0, \mathbf{k}_0)$ and close to the points (E_1, D_1, A_1) where $\sigma_2 k_2 \to \sigma_0 k_0 = 1$, the maximum gain is proportional to Σ/ε with $\varepsilon = 1 - \sigma_2 k_2/(\sigma_0 k_0)$, $\Sigma = 1 - \sigma_1 k_1/(\sigma_0 k_0)$ and the separatrix defining the edge of the different dynamics by a perturbation energy of order ε/Σ, the two being only function of k_1. Large transient growth and small threshold for the nonlinear stability (smallest perturbation to have the transition to a different state) then occur, the wave $(\omega_2, \mathbf{k}_2)$ playing the role of a repeller attracting for long time the dynamics of the system. In the rotating fluid, the secondary wave with wavevector nearly horizontal and vanishing frequency is associated to the geostrophic and quasi-geostrophic balance originating in the well-known Taylor column phenomenon where the motion in all three directions is uniform along the axis of rotation i.e. in an entire column of fluid. The transient growth of perturbation for linearly stable triads, and more importantly for nonlinear instability characterized by a small threshold amplitude to cross the separatrix, corresponds to the energy transfer between coupled inertial waves of finite amplitudes and arbitrary wavevectors, and small Taylor column motions of horizontal wavelength half that of the wave $(\omega_0, \mathbf{k}_0)$ in case E, and of long horizontal period in case D. In the case D, the secondary wave $(\omega_2, \mathbf{k}_2)$ is close to wave $(\omega_0, \mathbf{k}_0)$ since $(-\omega_0, -\mathbf{k}_0)$ and $(\omega_0, \mathbf{k}_0)$ represent the same wave and this transfer corresponds to a sideband instability whereas in the case E, the exchange of energy occurs with the secondary wave $(\omega_2, \mathbf{k}_2)$ identical to $(\omega_0, \mathbf{k}_0)$ but propagating in the opposite horizontal direction reproducing the periodic flip described for the tennis racket but here for wave in continuous liquid in rotation. As for the racket, the dynamics is given by the separatrix leading to the relaxation from one unstable state to its opposite. In this intermittent solution, the dynamics is led the majority of the time by the unstable state playing the role of a repeller, its stable and unstable manifold defining the edge state, here the separatrix.

GENERALIZATION TO TRIADIC WAVE RESONANCE

Triadic resonance is a generic feature of *any* systems where small amplitude solutions may be represented by a superposition of waves described by a dispersion relation $\mathcal{D}(\omega, \boldsymbol{k}) = 0$ and when the resonant condition (6) is fulfilled by three particular wavevectors $(\mathbf{k}_0, \mathbf{k}_1, \mathbf{k}_2)$.

As we already did for inertial waves, we follow Craik's derivation [12] in the two-dimensional case (2D) for a scalar state field q. The field q follows an equation involving non-linear quadratic terms $\hat{\mathcal{D}}(q) = \hat{\mathcal{N}}(q, q)$ where $\hat{\mathcal{D}}$ is a linear operator and $\hat{\mathcal{N}}$ a bilinear form [13]. This nonlinear equation is analyzed assuming the magnitude of q small enough of order ε by an asymptotic procedure introducing a multiscale expansion in time with a slow time $T = \varepsilon t$. Expanding q in ε with $q = \varepsilon q_1 + o(\varepsilon)$, we obtain at leading order in ε that $\hat{\mathcal{D}}(q_1) = 0$ whose solution is a superposition of waves $\exp i(k_{xn} x + k_{zn} z - \omega_n t)$ with an arbitrary amplitude $Q_n(T)$, function of the slow time scale only, and where $(\omega_n, \boldsymbol{k}_n)$ obey the dispersion relation $\mathcal{D}(\omega_n, \boldsymbol{k}_n) = 0$ deduced from the operator $\hat{\mathcal{D}}$. At second order in ε, waves respecting the triadic resonance condition (6) are coupled and when going back to the primitive time variable t (see [12] for more details), the compatibility condition for a particular triad reads $i\partial\mathcal{D}/\partial\omega_{|n} \times dQ_n/dt = \lambda_n Q_m^* Q_l^*$, (n, m, l) being any circular permutation of $(0, 1, 2)$, λ_n the nonlinear interaction coefficients, and $\partial\mathcal{D}/\partial\omega_{|n}$ is $\partial\mathcal{D}/\partial\omega$ evaluated at $(\omega_n, \boldsymbol{k}_n)$. λ_n and $\partial\mathcal{D}/\partial\omega_{|n}$ being both real. Rescaling the amplitudes Q_n by introducing $A_n = \kappa \left|\partial\mathcal{D}/\partial\omega_{|n}/\lambda_n\right|^{1/2} Q_n$, with the normalization factor $\kappa = -i \left|\lambda_0\lambda_1\lambda_2/\left(\partial\mathcal{D}/\partial\omega_{|0}\partial\mathcal{D}/\partial\omega_{|1}\partial\mathcal{D}/\partial\omega_{|2}\right)\right|^{1/2}$, leads to the generic three wave interaction equations:

$$\begin{aligned} \frac{dA_0}{dt} &= s_0 A_2^* A_1^* \\ \frac{dA_1}{dt} &= s_1 A_0^* A_2^* \\ \frac{dA_2}{dt} &= s_2 A_1^* A_0^* \end{aligned} \tag{10}$$

with the notations $s_n = \text{sign}\left(\partial\mathcal{D}/\partial\omega_{|n}\lambda_n\right)$. Two cases should be distinguished. In the first case, all signs s_n are identical, solutions of (10) may diverge at finite time, and this singularity, if it occurs, implies an explosive breakdown of the solution [14]. This case is frequent in plasma physics [8] and also possible in three-layer Kelvin-Helmholtz flow [15]. In the other case, s_n are different, solutions of (10) are bounded, which is the case of most waves in fluid at rest, like surface, interfacial and internal waves as discussed by [16] and [17]. Multiplying each line of (10) by A_n^* and adding the complex conjugate of the equation, we get $d\left|A_n\right|^2/dt = 2s_n\Re(A_0A_1A_2)$ leading to relations equivalent to the Manley-Rowe relations [18] :

$$\frac{d}{dt}(s_0\left|A_0\right|^2) = \frac{d}{dt}(s_1\left|A_1\right|^2) = \frac{d}{dt}(s_2\left|A_2\right|^2) \tag{11}$$

which imply the existence of two quadratic invariants $C_0 = s_1\left|A_1\right|^2 - s_2\left|A_2\right|^2$ and $C_1 = s_2\left|A_2\right|^2 - s_0\left|A_0\right|^2$, the third permutation being a combination of these two invariants $C_2 \equiv -C_0 - C_1 = s_0\left|A_0\right|^2 - s_1\left|A_1\right|^2$. These two invariants may be combined in infinitely many linear combinations, as for example for any three real coefficients $\alpha = (\alpha_0, \alpha_1, \alpha_2)$ such that $\alpha_0 + \alpha_1 + \alpha_2 = 0$, $\mathcal{B} = \sum_n s_n\alpha_n\left|A_n\right|^2$ is an integral of motion, but only in particular cases, some invariants $\mathcal{B}$, linked to a particular trinomial $\alpha = (\alpha_0, \alpha_1, \alpha_2)$, have a physical interpretation. For many classical cases of waves in a medium initially at rest, triadic resonance between waves conserves the total energy, sum of the kinetic and potential energy of the three waves. This physically conserved quantity correspond to a particular choice of trinomial $\alpha = (\alpha_0, \alpha_1, \alpha_2)$, but this choice is a priori complex since the normalization from the wave amplitudes Q_n to the rescaled amplitudes A_n depends on the form of the dispersion relation and on the nonlinear operator $\hat{\mathcal{N}}(q, q)$, and may be an intricate function of ω_n and $\boldsymbol{k}_n$. Still, in some particular cases as the one treated here (inertial waves [4]) and for capillary gravity waves [19], internal waves [20], waves in plasma [8], and the swinging spring [7], the normalization is such that choosing then $\alpha = (\omega_0, \omega_1, \omega_2)$, the three wave frequencies, leads to the energy invariant up to a normalization constant K_{triad} that depends on the considered triad, $\mathcal{E} = \sum_n s_n\omega_n\left|A_n\right|^2/K_{triad} = \sum_n \mathcal{E}_n$ [17], the energy of the n-th wave being $\mathcal{E}_n = s_n\omega_n\left|A_n\right|^2/K_{triad}$.

In the studied cases, choosing $\alpha = (k_{x0}, k_{x1}, k_{x2})$ gives the conservation of the x component of the pseudomomentum $p_x = \sum_n s_n k_{xn} |A_n|^2 / K_{triad} = \sum_n \mathcal{A}_n k_{xn}$ with the classical wave action $\mathcal{A}_n = s_n |A_n|^2 / K_{triad} = \mathcal{E}_n/\omega_n$ [21] up to the same normalization constant as for the energy K_{triad}. Similarly, $\alpha = (k_{z0}, k_{z1}, k_{z2})$ gives the conservation of the z component of the pseudomomentum $p_z = \sum_n s_n k_{zn} |A_n|^2 / K_{triad} = \sum_n \mathcal{A}_n k_{zn}$. However, we should insist on the fact that this direct matching between energy and wave action definitions with the invariants of (10) is not imposed by the present derivation given by choosing respectively the frequencies and the components of the wavevectors as the prefactor α_n, and should be specifically verified. In particular, we may remark that choosing $\alpha = (\omega_0 + ck_{x0}, \omega_1 + ck_{x1}, \omega_2 + ck_{x2})$, equivalent to a Doppler shift along the x direction, where c would be a uniform velocity, also leads to an invariant of equation (10), which would be the physical energy for an inertial wave, only if the fluid were not at rest but in a uniform motion at velocity $-c$ along the x direction.

As for inertial waves, equations (10) admit a third invariant linking the phase of the waves to their amplitudes, which imposes $\mathcal{K} = \Im(A_0 A_1 A_2)$ is constant in time, leading to the same equation for $\mathcal{K}$ as (9).

In the cases where the physical energy is such that $\mathcal{E} = \sum_n s_n \omega_n |A_n|^2 / K_{triad}$, all the results discussed for inertial waves apply, and the dynamics of resonating triads is characterized by the intersection of energy and pseudo-momentum ellipsoids. The distance measured in the energy norm between the separatrix, the unstable manifold of the unstable wave, and the stable wave with the closest pseudomomentum, depends only on the frequencies and wavevectors of the three waves in the triad. Relaxation oscillations may dominate in systems where this distance can become infinitely small for some particular triads. If subscript 2 indicates the unstable wave, 0 and 1 the stable ones as we did for inertial waves, relaxation oscillations dominate in triadic resonant systems achieving the condition that, on the unit energy ellipsoid, the x and z components of $\boldsymbol{p}_0 - \boldsymbol{p}_2$ are small compared to those of $\boldsymbol{p}_0 - \boldsymbol{p}_1$, with $\boldsymbol{p}_n = \boldsymbol{k}_n/\omega_n$ the pseudomomentum of the n-th wave at unit energy $\mathcal{E}_n = 1$. It is easy to show that the two vectors $\boldsymbol{p}_0 - \boldsymbol{p}_2$ and $\boldsymbol{p}_0 - \boldsymbol{p}_1$ are colinear and co-directed as a result of the definitions of energy and pseudomomentum on the separatrix, $\boldsymbol{p}_0 - \boldsymbol{p}_2 = \gamma \times (\boldsymbol{p}_0 - \boldsymbol{p}_1)$ with $\gamma > 0$, and that relaxation oscillations dominate if $\gamma \ll 1$. In terms of phase velocity of the n-th wave $\boldsymbol{c}_n = (c_{xn}, c_{zn}) = (\omega_n/k_{xn}, \omega_n/k_{zn})$, we have, when the denominator is not nil :

$$\gamma = \frac{c_{x0}^{-1} - c_{x2}^{-1}}{c_{x0}^{-1} - c_{x1}^{-1}} = \frac{c_{z0}^{-1} - c_{z2}^{-1}}{c_{z0}^{-1} - c_{z1}^{-1}} \quad (12)$$

that should be small for large transient growth of perturbation energy and relaxation oscillations to be present. Achieving this criterion depends solely on the form of the dispersion relation $\mathcal{D}(\omega, \boldsymbol{k}) = 0$ specific to the studied waves. In the case of inertial waves, those criteria can be simplified using the dispersion relation (5), and we show that the previous condition, $\gamma \ll 1$, is equivalent to $\sigma_2 k_2 \to \sigma_0 k_0$ for triads indicated by points (E_1, D_1, A_1) on figure 3, and $\sigma_1 k_1 \to \sigma_0 k_0$ for (E_2, D_2, A_2), hence recovering the main results of the previous part.

CONCLUSION AND DISCUSSION

The analogy between rotating solid and fluid is based on the conservation of two quadratic invariants : energy and momentum for the rotating solid, and energy and helicity for the triadic resonance of inertial waves in a rotating fluid. Both systems, when initially rotating around a stable mode and submitted to a perturbation of small but finite amplitude, exhibit high transient growth of perturbation energy and relaxation oscillations towards the unstable mode. Those dynamics are captured by the intersection of constant energy sphere and varying momentum ellipsoids in the solid case, and constant energy sphere and varying helicity ellipsoids for triadic resonant inertial waves.

The general case of resonant wave triads may be reduced to two cases depending on the three signs of the coupling coefficients. In the first case, these three coefficients have the same sign, the amplitude of the waves may grow unbounded. In the other case, a quadratic invariant of the motion corresponds to a definite positive form, preventing the solution to diverge to infinity. The stability of the three waves is then well-defined and studied, one wave being unstable and the other stable, for any finite amplitude initial condition. In many specific problems where the energy may be defined as a physically conserved quantity in the triads, the dynamics described for inertial waves applies with the possibility to define the energy of the perturbation around a single wave in the triads, the main result being that this departure from a single wave may exhibit large transient growth. In particular, for a a large class of systems such as capillary gravity waves [19], internal waves [20], waves in plasma [8], and the swinging spring [7], the conservation of energy and the properties of triadic interaction allow to define the pseudomomentum, by introducing the wave action, as we did for inertial waves, and to show that the pseudomomentum is also conserved. Then, for triads such that, at equal energy, the pseudo-momentum of the unstable wave 2 gets closer to that of the stable wave 0 than that of wave 1, the linear dynamics around the perturbed wave 0 exhibits strong transient growth of perturbation energy, and the distance in energy norm between the stable mode 0 and the separatrix (i.e. the stable manifold of wave 2) becomes small leading to relaxation oscillations towards the unstable wave 2.

Such dynamics may be evidenced experimentally in the solid case by taking inspiration from the experiment shown in the YouTube video mentioned in the introduction, which demonstrates the tennis racket effect by unscrewing a T-handle in zero gravity at the International Space Station, resulting in a spinning motion around its unstable axis with a periodic 180° twist. The T-handle is such that the screwed bar has the intermediate moment of inertia along the symmetry axis of the T. This moment is smaller, but close to the highest moment of inertia along the normal axis to the plane of the T, since the two differ by the moment of inertia of the vertical branch of the T, which is thin for the T-handle used. The third moment around the upper branch of the T is much smaller, since it involves mainly the rotation of the thin vertical branch. The present study predicts the dynamics of a solid object having its intermediate moment of inertia close to the greatest one when spinning such object around its stable axis of greatest moment of inertia. Such object could be shaped as an ellipsoid of semi-axes $a < b < c$ with $b \to a$ and scratched on its axis of greatest moment of inertia a to distinguish it from the intermediate axis b indicated by a dot. In zero gravity, we may spin this ellipsoid around the stable axis a, scratched, and, for a small perturbation, we expect to observe a growth of the perturbation and a rapid reorientation of the rotation from this stable axis, toward the unstable one b indicated by the dot. The solid should then keep spinning around the unstable axis b (dotted) for a large time with relaxation oscillations, where the rotation axis turns and passes close to the stable axis a (scratched) before finishing the 180° flip rotating along the unstable axis, but in the opposite direction and so on and so forth.

This YouTube video also shows a second experiment under zero gravity condition. A liquid-filled cylinder, initially spinning around its stable axis of smallest moment of inertia, becomes unstable, and the cylinder ends up rotating around its stable axis of greatest moment of inertia. The physical interpretation proposed is that the inner fluid adds the possibility of dissipation of energy, effective as soon as a small nutation is imposed in the initial condition, and as this viscous fluid motion dissipates energy leading to the destabilization of the stable axis with transfer of momentum towards the direction with the largest inertia. This phenomenon was already described by Lord Kelvin in his 1880 paper in Nature on the difference of stability in the dynamics of a liquid-filled gyroscope with a slight prolate ovoidal shape [22]. He attributed this difference to the property of the support:

> *The rotation of a liquid in a rigid shell of oval figure, being a configuration of maximum energy for given vorticity, would be unstable if the containing vessel is left to itself supported on imperfectly elastic supports, although it would be stable if the vessel were held absolutely fixed, or borne by perfectly elastic supports, or left to itself in space unacted on by external force.*

This physical interpretation may be partial, since the destabilization of the stable axis of the solid may not only be due to dissipation or to the holding support properties, but also to the coupling with internal degrees of freedom in the fluid. Indeed, the nutation and precession of the solid filled with a liquid have been shown to excite inertial waves [23] via resonance mechanisms, similar to triadic interaction, involving the destabilization of the secondary flow induced by the solid motion. Instead of the viscous damping of this secondary flow, its coupling with resonnant internal wave would add to equations (1) other degrees of freedom, corresponding to secondary wave amplitudes, able to change the stability properties of the initial condition of a pure solid body rotation along the axis of smallest moment of inertia. Such system remains to be derived and explored.

Though the dynamics described in this second experiment is quite different from the one described in the present article (as the liquid introduces extra degrees of freedom and adds internal dissipation), the same experiment could be adapted with a spinning liquid-filled ellipsoid of semi-axes $a < b < c$ with $b \to a$, same as before (scratched on the a axis and dotted on the b axis). We may conjecture that adding an inner fluid should suppress the relaxation oscillations around a. Experimental evidences of the dynamics predicted here is not straightforward, but we may suggest that, for a rotating fluid in an infinite domain, the present model predicts that, in the presence of a weak mode with nearly zero frequency, characterized by columns of fluid moving in a vertically nearly uniform way (Taylor columns), any wave moving vertically up will progressively transfer its energy to a similar wave moving down and back again.

[1] L. Van Damme, P. Mardešić, and D. Sugny, Physica D **338**, 17 (2017)

[2] L. Euler, Memoires de l'academie des sciences de Berlin **8**, 154 (1758)

[3] H. K. Moffatt, J. Fluid Mech. **741**, R3 (2014)

[4] G. Bordes, F. Moisy, T. Dauxois, and P. Cortet, Phys. Fluids **24**, 014105 (2012)

[5] C. M. Bender and S. A. Orszag, in *Advanced Mathematical Methods for Scientists and Engineers I: Asymptotic Methods and Perturbation Theory*, edited by C. M. Bender and S. A. Orszag (Springer, New York, NY, 1999) pp. 484–543

[6] L. M. Smith and F. Waleffe, Phys. Fluids **11**, 1608 (1999)

[7] P. Lynch, Bull. Amer. Meteor. Soc. **84**, 605 (2003)

[8] J. Weiland and H. Wilhelmsson, Pergamon Press **88** (1977)

[9] T. M. Schneider and B. Eckhardt, Philos. Trans. R. Soc. A **367**, 577 (2009)

[10] K. Hasselmann, J. Fluid Mech. **30**, 737 (1967)

[11] C. H. McComas and F. P. Bretherton, J. Geophys. Res. **82**, 1397 (1977)

[12] A. D. D. Craik, *Wave interactions and fluid flows*, Cambridge monographs on mechanics and applied mathematics (Cambridge University Press, Cambridge [Cambridgeshire] ; New York, 1985)

[13] W. Eckhaus, *Studies in Non-Linear Stability Theory*, Springer Tracts in Natural Philosophy (Springer-Verlag, Berlin Heidelberg, 1965)

[14] B. Coppi, M. N. Rosenbluth, and R. N. Sudan, Annals of Physics **55**, 207 (1969)

[15] A. D. D. Craik and J. A. Adam, J. Fluid Mech. **92**, 15 (1979)

[16] F. K. Ball, J. Fluid Mech. **19**, 465 (1964)

[17] T. Joyce, J. Fluid Mech. (1974)

[18] J. M. Manley and H. E. Rowe, Proc. IRE **44**, 904 (1956)

[19] L. F. McGoldrick, J. Fluid Mech. **21**, 305 (1965)

[20] R. E. Davis and A. Acrivos, J. Fluid Mech. **30**, 723 (1967)

[21] G. B. Whitham, J. Fluid Mech. **22**, 273 (1965)

[22] W. Thomson, Nature **23**, 69 (1880)

[23] M. Le Bars, D. Cebron, and P. Le Gal, Annu. Rev. of Fluid Mech. **47**, 163 (2015)